CHAPTER 130

FORCES ON VERTICAL WALLS DUE TO OBLIQUELY-INCIDENT WAVES

Ching-Piao Tsai * and Dong-Sheng Jeng **

Abstract

The force exerted on a vertical wall due to obliquely-incident waves has been analyzed in this paper from the calculation of short-crested waves system by a numerical scheme. The numerical model preserves the wave elevation in an implicit function form for the dynamic and kinematic boundary equations on water surface, the accuracy is then improved. It is found that the maximum loading in onshore direction may be caused by obliquely-incident waves as the water is greater than intermediate depth. However, the onshore loading does not necessarily be the greatest force for such instance. The greatest force could be produced by the offshore loading under steeper normal standing waves. While the wall is in the shallow water region, the greatest force is occurred in onshore loading at crest by normal standing waves. This research also shows good comparisons from some experimental results.

1. Introduction

Wave forces exerted on vertical walls play a very important role in coastal engineering. The forces produced by standing waves, whose crest parallel to the wall, are usually considered as the maximum loads. However, some evidences have shown that the forces due to obliquely-incident waves, called short-crested waves, could exceed those from waves normal approach to the wall (Silvester 1974, Fenton 1985). The surface of short-crested wave is defined as having a doubly-periodic diamond-shaped crest pattern. Two dimensional progressive and standing waves are physically two limiting cases of short-crested waves as the incident waves are traveling parallel and normal to the wall respectively.

Short-crested waves have been investigated theoretically since Fuchs (1952). The systematic analysis by a third-order approximation in a non-dimensional form was proposed by Hsu et al (1979). While the detailed analysis for the force on vertical walls due to such wave system was first studied by Fenton (1985), with a third-order expansion in wave height. Fenton's solutions showed a number of unusual features which can further be found in this study. Nevertheless, it is found that the third-order

* Associate Professor, Department of Civil Engineering, National Chung-Hsing University, Taiwan 40227, Republic of China
** Master of Engineering, Department of Civil Engineering, National Chung-Hsing University, Taiwan 40227, Republic of China

approximation could produce moderately residual pressures on free surface, which has an influence on the distribution of wave pressures, as the wave is in shallow water, or steeper in intermediate depth in which coastal structures are always located.

To improve the accuracy, the force exerted on a vertical wall is obtained in the study from calculation short-crested waves by a numerical scheme. The numerical model using Fourier series approximation was proposed to calculate the highest periodic short-crested waves on deep water by Tsai et al (1990). Unlike Roberts and Schwartz (1983), the present numerical model preserves the wave elevation function in an implicit form, in analogy to the exact nonlinear nature for the dynamic and kinematic boundary conditions on water surface. Basic formulations are outlined in section 2, and the main procedures for numerical calculations given in section 3. Section 4 demonstrates the results of the force exerted on the wall. The experimental data of standing waves (Goda 1967), one of limiting cases of short-crested waves, are also quoted to compare with the calculation results.

2. Formulations

A sketch diagram of the short-crested wave motion produced by full oblique reflection from a vertical wall is shown in Fig. 1. Assume the fluid to be inviscid, incompressible and of uniform finite depth. The velocity potential ϕ for irrotational motion gives rise to the Eulerian water particle velocity components as

$$u=\phi_x, \ v=\phi_y, \ w=\phi_z \tag{1}$$

where the velocity potential $\phi(x,y,z,t)$ satisfies Laplace equation

$$\nabla^2\phi = \phi_{xx} + \phi_{yy} + \phi_{zz} = 0 \tag{2}$$

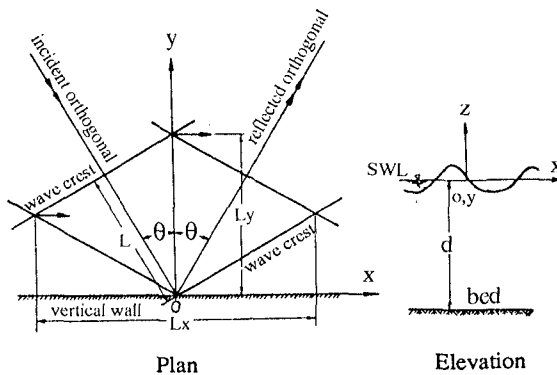The dynamic boundary condition at the free surface (DFSBC) is

Fig. 1 Sketch diagram of short-crested waves

$$\phi_t + g\eta + \frac{1}{2}(\phi_x^2 + \phi_y^2 + \phi_z^2) = C, \quad \text{at } z = \eta \tag{3}$$

and the kinematic boundary condition at the free surface (KFSBC) is

$$\eta_t - \phi_z + \phi_x\eta_x + \phi_y\eta_y = 0, \quad \text{at } z = \eta \tag{4}$$

while the bottom and wall boundary conditions are

$$\phi_z = 0 \quad \text{at } z = -d; \quad \phi_y = 0 \quad \text{at } y = 0 \tag{5}$$

in which $\eta = \eta(x,y,t)$ is the water surface elevation, g is the acceleration due to gravity, and the subscripts (x,y,z ,t) designate differentiation with respect to the Cartesian co-ordinates (see Fig.1) and the time, and C is an arbitrary constant.

Taking the material derivative, D/Dt, of (3) and subtracting g times (4) gives

$$\phi_{tt} + g\phi_z + 2(\phi_x\phi_{xt} + \phi_y\phi_{yt} + \phi_z\phi_{zt}) + 2(\phi_x\phi_y\phi_{xy} + \phi_x\phi_z\phi_{xz} + \phi_y\phi_z\phi_{yz})$$

$$+ (\phi_{xx}\phi_x^2 + \phi_{yy}\phi_y^2 + \phi_{zz}\phi_z^2) = 0 \quad \text{at } z = \eta \tag{6}$$

The unknown time derivative of η_t in (4) can thus be eliminated, in which η is a priori unknown itself yet to be determined.

As shown in Fig.1, let L be the wavelength of the incident and reflected waves and L_x and L_y the distances between crests in the x and y directions respectively. The corresponding components of the wavenumber k in these two directions may be defined as

$$k_x = 2\pi / L_x = k\sin\theta = pk, \quad k_y = 2\pi / L_y = k\cos\theta = qk \tag{7}$$

in which $k = 2\pi / L$. By using a reference length 1/k and reference time $1/\sqrt{gk}$, the following set of non-dimensional parameters may be introduced,

$$\hat{x} = pkx - \sigma t, \quad \hat{y} = qky, \quad \hat{z} = kz$$

$$\hat{\phi} = \frac{k^2}{\sqrt{gk}}\phi, \quad \hat{\eta} = k\eta, \quad \omega = \frac{\sigma}{\sqrt{gk}} \tag{8}$$

in which σ is the angular frequency of the incident and reflected wave (i.e. $\sigma = 2\pi / T$ where T is the wave period in seconds).

The carets denoting dimensionless quantities will now be omitted for the sake simplicity, unless otherwise specified. The governing equations may now be transformed in terms of these dimensionless quantities.

$$p^2\phi_{xx} + q^2\phi_{yy} + \phi_{zz} = 0 \tag{9}$$

$$-\omega\phi_x + \eta + \frac{1}{2}(p^2\phi_x^2 + q^2\phi_y^2 + \phi_z^2) = Q, \quad \text{at } z = \eta \tag{10}$$

$$\omega^2\phi_{xx} + \phi_z - 2\omega(p^2\phi_x\phi_{xx} + q^2\phi_y\phi_{xy} + \phi_z\phi_{xz})$$

$$+ 2(p^2q^2\phi_x\phi_y\phi_{xy} + p^2\phi_x\phi_z\phi_{xz} + q^2\phi_y\phi_z\phi_{yz})$$

$$+ (p^4\phi_{xx}\phi_x^2 + q^4\phi_{yy}\phi_y^2 + \phi_{zz}\phi_z^2) = 0, \quad \text{at } z = \eta \tag{11}$$

$$\phi_z = 0 \quad \text{at } z = -d \tag{12}$$

$$\phi_y = 0 \quad \text{at } y = 0 \tag{13}$$

in which Q is a dimensionless constant.

3. Numerical procedures

A truncated double Fourier series which satisfies both Laplace equation (9) and the bottom and wall boundary conditions (12) and (13) can be given by

$$\phi = \sum_{m=1}^{M-1} \sum_{n=0}^{2N} B_{mn} \frac{\cosh \alpha_{mn}(z+d)}{\cosh \alpha_{mn} d} \sin mx \cos ny \tag{14}$$

in which $\alpha_{mn}^2 = p^2m^2 + q^2n^2$. As $(m+n)$ is odd, then B_{mn} is equal to zero for satisfying the symmetry condition required for the wave motion. The equation (14) yields the appropriate two-dimensional limiting cases of a progressive wave as $p=1$ and $q=0$, and a normal standing wave when $p=0$ and $q=1$. Substituting (14) into DFSBC (10) and KFSBC (11), yields

$$-\omega u + \eta + \frac{1}{2}(p^2u^2 + q^2v^2 + w^2) = Q \tag{15}$$

and

$$\omega^2 u_x + w - 2\omega(p^2u_xu + q^2u_yv + u_zw) + 2(p^2uu_zw + p^2q^2uu_yv + q^2 vv_zw)$$

$$+ (p^4u_xu + q^4v_yv^2 + w_zw^2) = 0 \tag{16}$$

where

$$u = \sum_{m=1}^{M-1} \sum_{n=0}^{2N} mB_{mn}F_{mn}(\eta) \cos mx \cos ny \qquad v = \sum_{m=1}^{M-1} \sum_{n=0}^{2N} -nB_{mn}F_{mn}(\eta) \sin mx \sin ny$$

$$w = \sum_{m=1}^{M-1} \sum_{n=0}^{2N} \alpha_{mn}B_{mn}G_{mn}(\eta) \sin mx \cos ny \qquad u_x = \sum_{m=1}^{M-1} \sum_{n=0}^{2N} -m^2B_{mn}F_{mn}(\eta) \sin mx \cos ny$$

$$u_y = \sum_{m=1}^{M-1} \sum_{n=0}^{2N} -mn B_{mn} F_{mn}(\eta) \cos mx \sin ny \qquad u_z = \sum_{m=1}^{M-1} \sum_{n=0}^{2N} m\alpha_{mn} B_{mn} G_{mn}(\eta) \cos mx \cos ny$$

$$v_y = \sum_{m=1}^{M-1} \sum_{n=0}^{2N} -n^2 B_{mn} F_{mn}(\eta) \sin mx \cos ny \qquad v_z = \sum_{m=1}^{M-1} \sum_{n=0}^{2N} -n\alpha_{mn} B_{mn} G_{mn}(\eta) \sin mx \sin ny$$

$$w_z = \sum_{m=1}^{M-1} \sum_{n=0}^{2N} \alpha_{mn}^2 B_{mn} F_{mn}(\eta) \sin mx \cos ny$$

$$F_{mn}(\eta) = \frac{\cosh \alpha_{mn}(\eta+d)}{\cosh \alpha_{mn}d} \qquad G_{mn}(\eta) = \frac{\sinh \alpha_{mn}(\eta+d)}{\cosh \alpha_{mn}d} \qquad (17)$$

It is noted that the water surface elevation $\eta(x,y)$ is preserved in an implicit form, instead of a straight double Fourier series by Roberts and Schwartz (1983). This approach is similar to that of Rienecker and Fenton (1981) in solving the problem of two-dimensional progressive waves.

For the purpose of numerical computations, the discretized mesh points (x_i, y_j) are chosen by even symmetric properties given by

$$x_i = i \pi / M , \qquad \text{for } i = 0,1,2,.....,M$$

$$y_j = j \pi / 2N, \qquad \text{for } j = 0,1,2,.....,N \qquad (18)$$

For all the mesh points required in (18), the DFSBC of (15) provides $(M+1)(N+1)$ algebraic equations. While (16) is automatically satisfied at points $(x_{M/2}, y_N)$, (x_0, y_j), and (x_M, y_j) for all j, and the value of (16) at points (x_{M-i}, y_N) are equal to that of (x_i, y_N) (for i=1,2,.....,M/2-1) from trigonometric symmetry. Then satisfied (16) at remaining points lead to $(M-1)N+M/2-1$ equations. Furthermore, there are two additional equations should be specified, firstly, a wave height relationship ensures that,

$$\eta_{00} - \eta_{M0} - H = 0 \qquad (19)$$

where η_{ij} represents $\eta(x_i, y_j)$, H is the waveheight of the short-crested wave. Secondly, the mean water level can be chosen at the coordinate origin, using the simple trapezoidal rule then

$$\frac{\pi^2}{8MN} \sum_{i=0}^{M-1} \sum_{j=0}^{N-1} (\eta_{ij} + \eta_{i+1\ j} + \eta_{i\ j+1} + \eta_{i+1\ j+1}) = 0 \qquad (20)$$

Consequently, there are $2MN+3M/2+2$ nonlinear algebraic equations for the same number of unknowns $B_{mn}, \eta_{ij}, \omega, Q$. The system equations can be solved by Newton's iteration scheme. It is noted that M should be taken to be an even integer.

4. Numerical results

Through the numerical scheme stated above, the velocity potential ϕ and wave elevation η of short-crested waves can be calculated completely as both the waveheight and water depth are given. The force exerted on the wall by short-crested waves, produced by obliquely-incident waves reflection from a vertical wall, then may be estimated by integrating the pressure over depth per unit of the wall. The pressure in the wave motion is given by Bernoulli's theorem in terms of dimensionless quantities as

$$\widehat{P} = -z - \omega\phi_x - \frac{1}{2}(p^2\phi_x^2 + q^2\phi_y^2 + \phi_z^2) + Q \tag{21}$$

where $\widehat{P} = (k/\rho g)P$ is the departure of the wave pressure from that of the atmosphere, ρ being the water density. The force on the wall per unit length due to the wave then performed by

$$F = \int_{-d}^{\eta} P(x, 0, z, t)\, dz \tag{22}$$

Considerring the hydrostatic contribution of the undisturbed water back of the wall, the net force on the wall per unit length then given by

$$[F] = \int_{-d}^{\eta} P(x, 0, z, t)\, dz - \frac{1}{2}\rho g d^2 \tag{23}$$

In the following results, the term M=2N=8 is taken to calculate. Since the wave elevation is preserved in an implicit form in the numerical model, the accuracy can be improved. The accuracy could be measured from the order of residual pressures (the non-zero value of pressures) on the water surface. Although the solution by traditional perturbation method was also obtained from satisfying the conditions of zero-pressure and continuity at the water surface, the pressure computed with the final solution does not necessarily become null at the surface due to the influence of higher order terms neglected in the calculation (Goda 1967). The error is especially occurred in the case of steeper wave in shallow water. In the numerical calculation of present model, however, the error less than 10^{-12} can be under control. Fig. 2 and Fig. 3 show that comparisons of the residual surface pressure / waveheight, in dimensionless $\widehat{Pr} / \widehat{H}$, of the steeper wave in the shallow water depth.

The variation of forces in each phase with different angle of incidence are shown in Fig. 4 and Fig. 5, the double peaks appear in small incident angle, such as $0°$, $5°$. But the phenomenon can not be found in the cases of shallow water and the small steepness in intermediate water depth, which are shown in Fig. 6 and Fig. 7 respectively. From the results, the maximum onshore force does not at the crest but at the intermediate maximum as the wave is small angles of incidence in deep water or larger steepness in intermediate water.
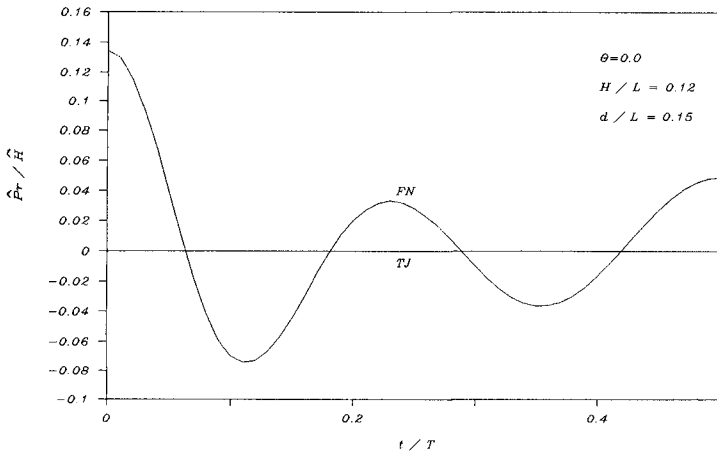
Fig.2   Variations of residual surface pressures with phase of time
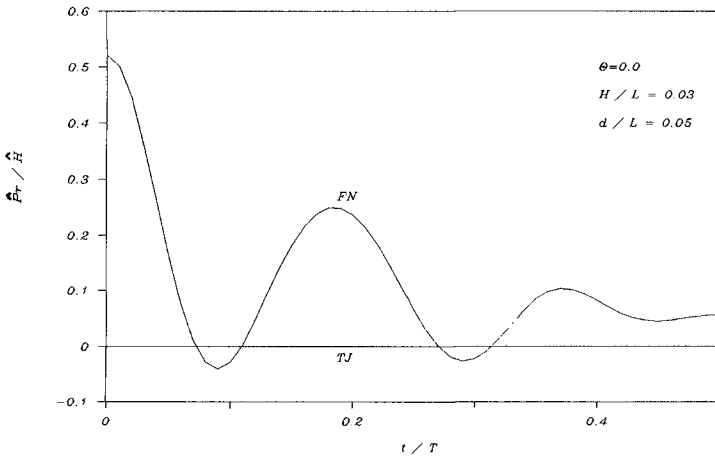TJ= Tsai & Jeng (present)   FN= Fenton (1985)

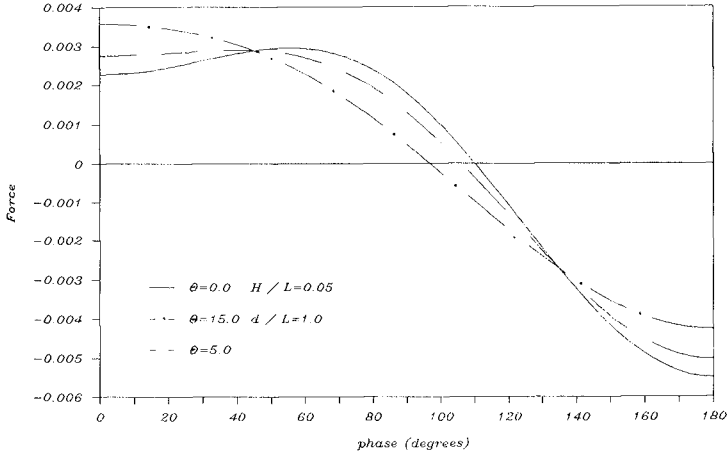Fig.3 Variations of residual surface pressures with phase of time

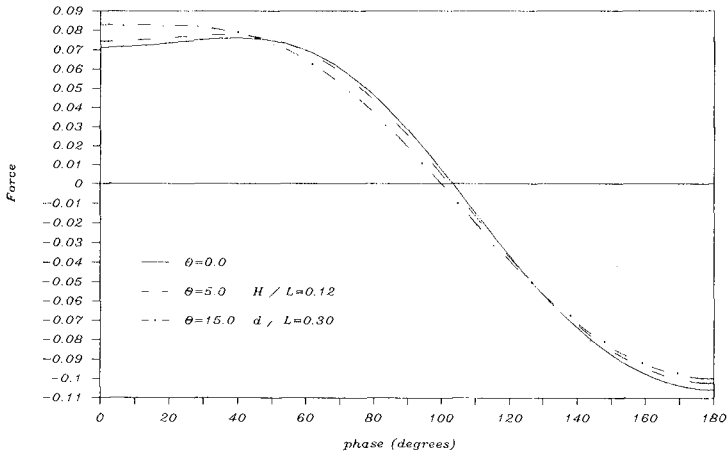Fig.4 Variation of forces in each phase, Force=[F] / ρgd^2

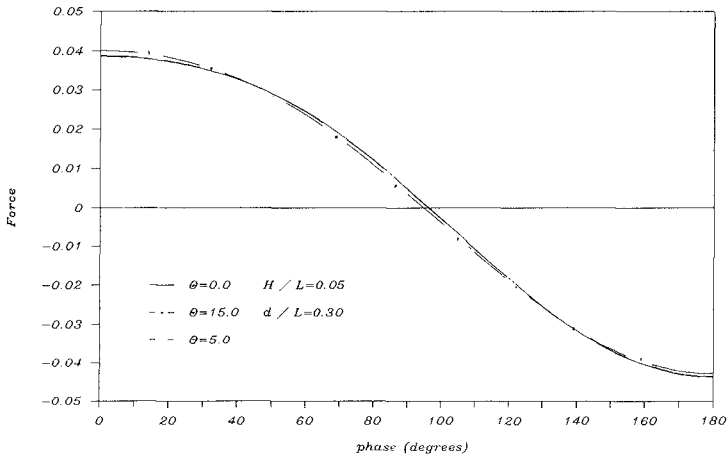Fig.5 Variation of forces in each phase, Force=[F] / ρgd^2

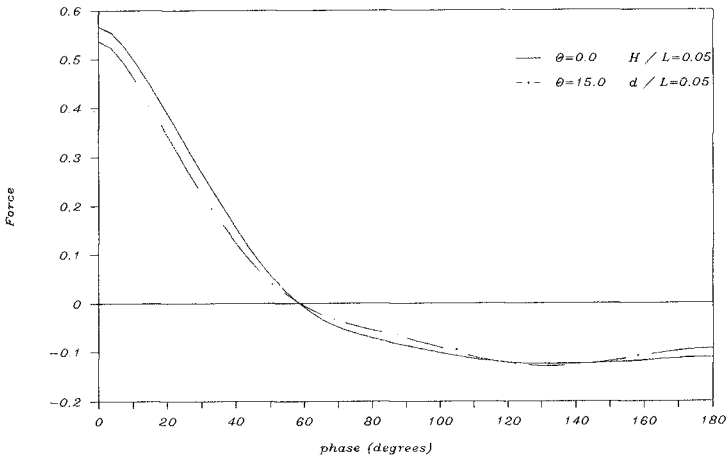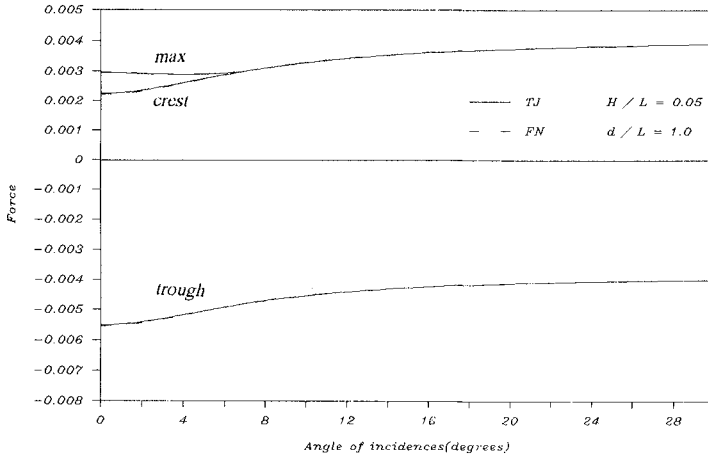Fig.6 Variation of forces in each phase, Force=[F] / $\rho g d^2$

Fig.7 Variation of forces in each phase, Force=[F] / $\rho g d^2$

Fig.8 Variation of forces with angle of incidence, Force=[F] / $\rho g d^2$
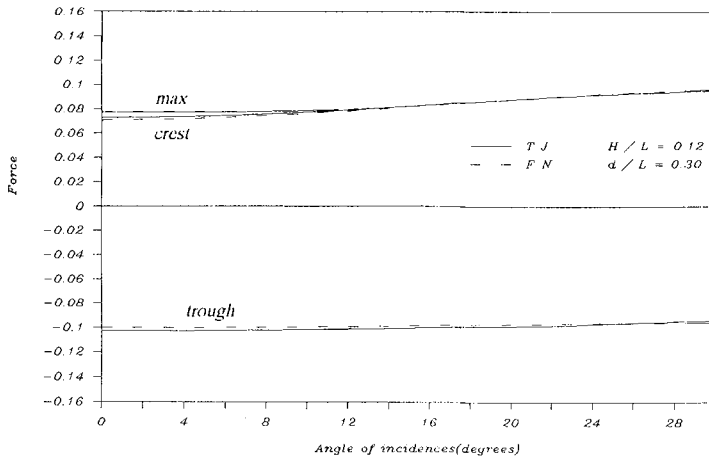

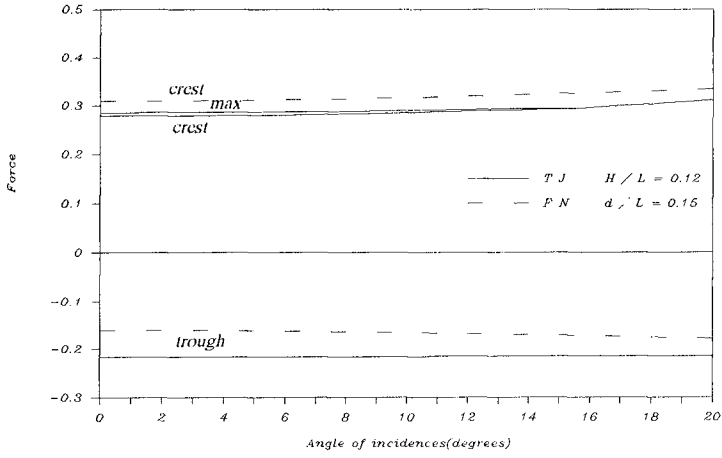Fig.9 Variation of forces with angle of incidence, Force=[F] / $\rho g d^2$

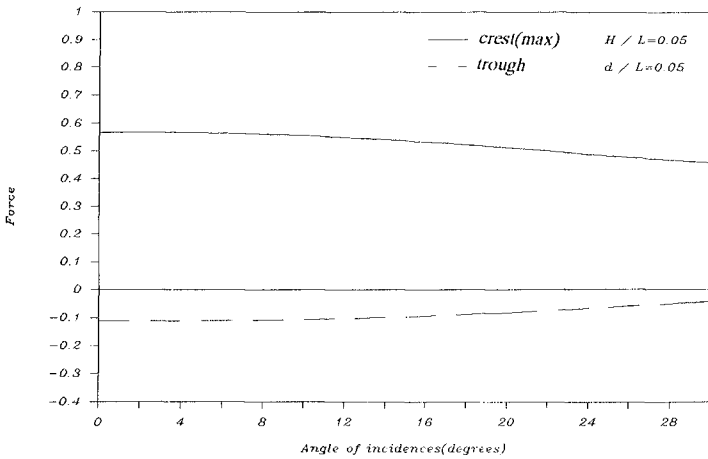Fig.10 Variation of forces with angle of incidence, Force=[F] / $\rho g d^2$

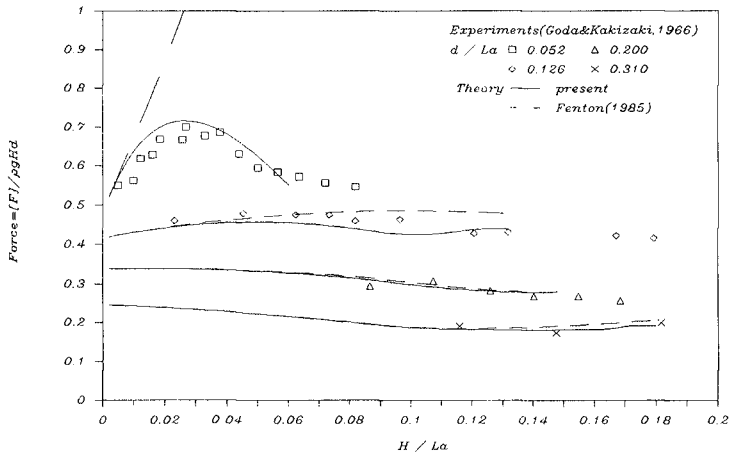Fig.11 Variation of forces with angle of incidence, Force=[F] / $\rho g d^2$

Fig.12   Comparison of maximum onshore wave force, Force=[F] / ρgdH
(La : wavelength of linear approximation)

Fig. 8 to Fig. 11 show the variation of forces per unit length with angle of incidence for each of the wave crest, the trough and the intermediate maximum. Analogous to Fenton (1985), the maximum force for onshore loading may be caused by obliquely-incident waves rather than standing waves. But this behavior is only found to be in water greater than intermediate depth, and opposite in shallow water. These figures also show the greatest net force exerted on vertical walls is occurred in offshore direction under the wave trough, as the water depth is greater than intermediate. And the maximum offshore loading is always produced by normal standing waves. Fig. 12 is the comparison from experimental data of the maximum onshore wave force of standing waves obtained by Goda (1967). The present research shows good agreement with experimental results even though the case of shallow water.

5. Conclusions

Through the calculation of short-crested waves by a numerical model, the force exerted on a vertical wall due to obliquely-incident waves has been obtained. Analogous to Fenton (1985), a number of unfeatures are also found in this paper. Because the wave elevation is preserved in an implicit function form for the dynamic and kinematic boundary equations on water surface, the results in this research show better agreement with some experimental data. Some conclutions can be drawn as the following. As the wave is in the water greater than intermediate depth, the double peaks appear on the time histories of forces in the cases of small incident angle. It is shown that the maximum loading in onshore direction does not be at the crest. From the analysis, it is also investigated that the maximum onshore loading may be caused by obliquely-incident waves rather than those of normal standing waves. Nevertheless, the maximum onshore loading does not necessarily be the greatest force for such instance. The greatest force is always produced by the offshore loading under the wave trough for normal standing waves as waves are steeper. While for shallow water waves, the greatest force is found in onshore loading at crest for normal standing waves.

Acknowledgement

References

Fenton, J.D. (1985) Wave forces on vertical walls. *J. Waterway, Port, Coastal and Ocean Engr., ASCE*, 111(4), 693-719.
Fuchs, R.A. (1952) On the theory of short-crested oscillatory. *Gravity Waves*, U.S. Nat. Bur. Stand. circular 521, 187-200.
Goda, Y. (1967) The forth order approximation to the pressure of standing waves. *Coastal Engineering in Japan*, 10, 1-11.
Hsu, J.R.C., Tsuchiya, Y. and Silvester, R. (1979) Third-order approximation to short-crested waves. *J. Fluid Mech.*, 90, 179-196.
Rienecker, M.M. and Fenton, J.D. (1981) A Fourier approximation of Stokes expansion of gravity waves. *J. Fluid Mech.* 104, 119-137.
Roberts, A.J. and Schwartz, L.W. (1983) The calculation of nonlinear short-crested gravity waves. *Phy. Fluid*, 26(9), 2388-2392.
Silvester, R. (1974) *Coastal Engineering*, Vol. I, Elsevier, Amsterdam, Netherlands.
Tsai, C.P., Jeng, D.S. and Hsu, J.R.C. (1990) Numerical calculation of the highest periodic short-crested waves on deep water. (to be published)